Electronic Supplementary Material (ESI) for Nanoscale.

Supplementary Information

Passive membrane penetration by ZnO nanoparticles is driven by the interplay of electrostatic and phase boundary forces

Anuj Tiwari[1], Ashutosh Prince[1]*, Manoranjan Arakha[1]*, Suman Jha[1], Mohammed Saleem[1†]

[1]Department of Life Sciences, National Institute of Technology, Rourkela, India - 769008

* equal contribution

Supporting text

Characterisation of ZnONP

Initially, the synthesis of ZnONP was confirmed by observing the surface plasmon resonance (SPR) property of ZnONP. As shown in Fig. 1a, the UV-Vis absorption peak of ZnONP which arises due to SPR property of the nanomaterial, was found to be at 367, which is in accordance with the results obtained by various groups.[1, 2] The energy band gap (E_{bg}) of synthesized ZnONP was evaluated using the equation, $E_{bg}=1240/\lambda$ (eV)[1] where E_{bg} and λ represent energy band gap in eV and cut-off wavelength in nanometre, respectively. The energy band gap of ZnONP was found to be 3.37 eV. The X ray diffraction (XRD) data (Fig. 1b) of ZnONP suggested that the synthesized ZnONP was crystalline in nature with diffraction peaks at 2θ angle values like 31, 34, 36, 47, 56, 62, 66, 67 and 68 correspond to different indices such as (100), (002), (101), (102), (110), (103), (200), (112) and (201), respectively. As reported, the obtained indices are well indexed to the hexagonal wurtzite structure of ZnO.[1] Additionally, the analysis of XRD spectra of ZnONP using X' pert high score software demonstrated that the synthesized ZnONP has hexagonal ZnO crystals (JCPDS reference code–80-0074). The average particle size of ZnONP was evaluated using Scherrer's equation:

$$\text{Particle size} = K*\lambda/\beta*\cos$$

Where λ and K represent the wavelength of X-ray ($1.540*10^{-10}$ m) and shape factor (0.9). Additionally, θ and β represent the Braggs angle and full width at half maximum. Using the above equation, the theoretical particle size was calculated to be 24 nm. The Fig.1c showed the surface potential of ZnONP which was found to be 19.1 mV. The morphological feature of the obtained ZnONP was further explored using TEM (Fig. 1d.), which demonstrated that most of the ZnONP are spherical in shape having a size range of ~ 25 ±10 nm.

Determination of the fluorescein-labeling ratio

As adapted from Menendez Miranda et al.[3]

For theoretical calculation of labeling ratio, we assume ZnO nanoparticle of 25nm diameter.

Considering the nanoparticle as a sphere. The volume of a single nanoparticle would be

$$V_{NP} = \frac{4}{3}\pi(r)^3 \quad \text{…. (1)}$$

Where, V_{NP} is the volume of one nanoparticle; π is 3.14 and r is radius of single nanoparticle.

Which comes to 8184.375 nm^3

Mass of total NP in solution= 1mg

Specific density of ZnONP = 5.606 g/cm^3 Arakha et al.

$$V_{TNP} = \frac{m}{specific\ density} \quad \text{…. (2)}$$

where, V_{TNP} is total volume of nanoparticle in solution, and m is the mass of nanoparticles in solution.

Which comes to 1.783 x 10^{-4} cm^3

$$T_{NP} = \frac{V_{TNP}}{V_{NP}} \quad \text{…. (3)}$$

Where, T_{NP} is total number of nanoparticles.

Which comes to 2.18 x 10^{13}

Therefore, the concentration of nanoparticle, C_{NP} in the solution will be calculated as-

$$C_{NP} = \frac{\frac{T_{NP}}{N_A}}{V} \quad \text{....(4)}$$

Where, N_A is Avagadro's number and V is total volume of solution in which nanoparticle is dissolved.

Concentration of NP comes to around 36nM

The concentration of Fluorescein in Fluorescein-NP calculated by the Beer-Lambert law = 2.3μM

The Fluorophore/NP ratio comes to ~ 63, which, is in line with previous report.

Technical details of dipole potential measurements

For dipole potential measurements it is reported by Gross et.al.,[4] that depending upon the changes in electric field in the surrounding of the potentiometric probe, it undergoes shift in the fluorescence excitation spectrum. This spectral shift is related to a corresponding change in the dipole potential:

$$\Delta v = \left(-\frac{1}{h}\right)\Delta\mu E - \left(\frac{1}{2h}\right)\Delta\alpha E^2$$

where, $\Delta\mu$ is the change in the electric dipole moment of the probe upon electronic excitation, $\Delta\alpha$ is the change in polarizability of the probe upon excitation, E is the electric field vector at the location of the chromophore and h is the Planck's constant. The first term describes frequency changes that depend linearly on the electric field and is dominant contribution for the field strengths that pertain in biological membranes. The relationship between the spectral shift and potential is, therefore, linear.

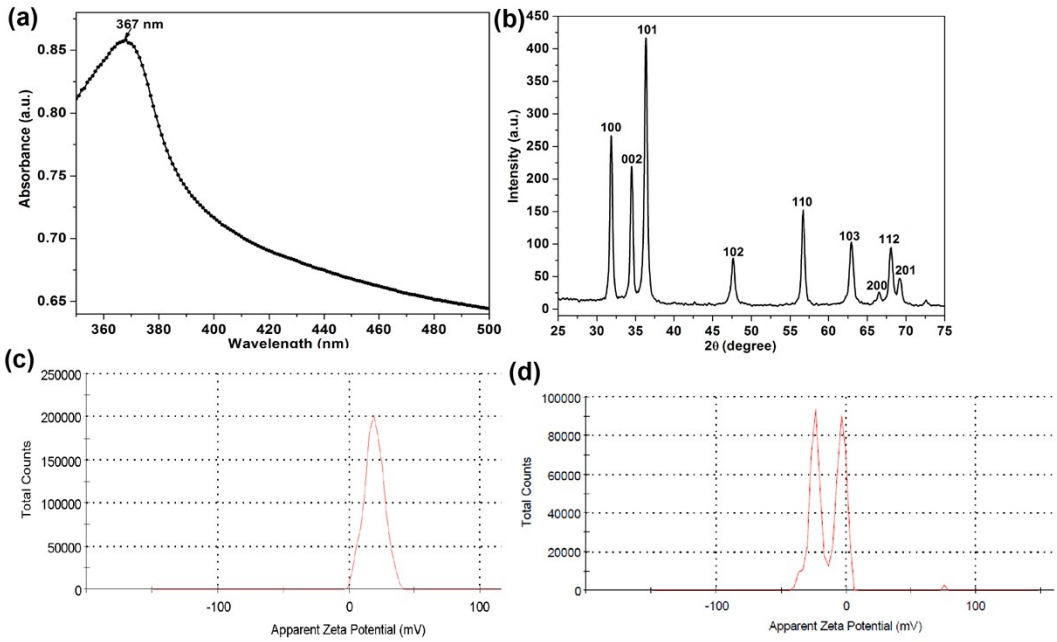

Figure S1: Characterization of ZnONP.

(a) UV-Vis absorption spectra of ZnONP (b) XRD spectra of ZnONP, (C) zeta potential analysis of ZnONP showing value of 19.1 mV, (d) Fluorescein ZnONP showing two populations of zeta potential with -13.6 mV

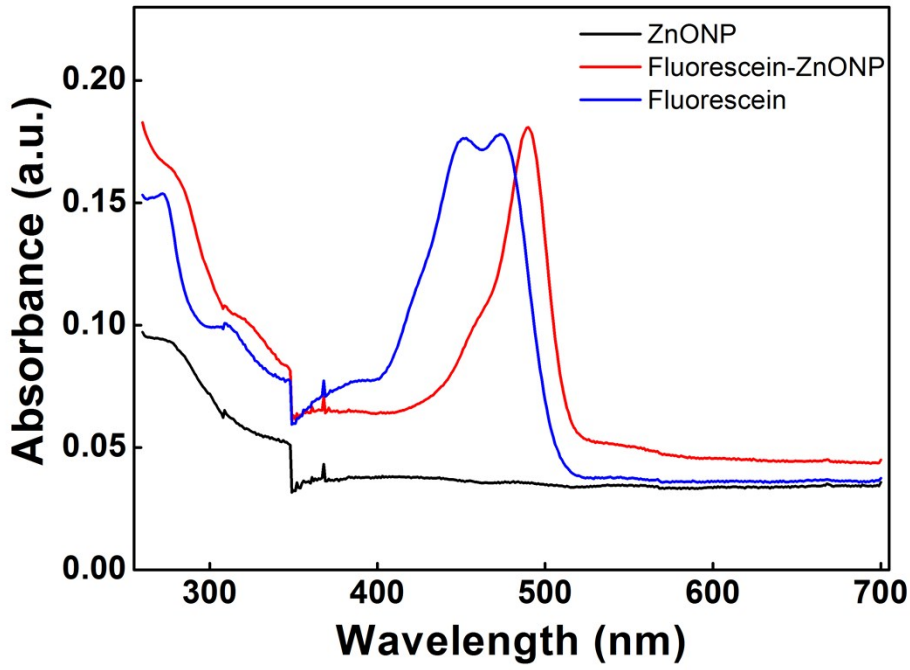

Figure S2: Absorbance of ZnONP, fluorescein-ZnONP and fluorescein.

A shift in the Absorption maxima of Fluorescein-ZnONP towards low energy due electronic interaction between Fluorescein and ZnONP confirms stable tethering of fluorescein to ZnONP by ionic interactions.

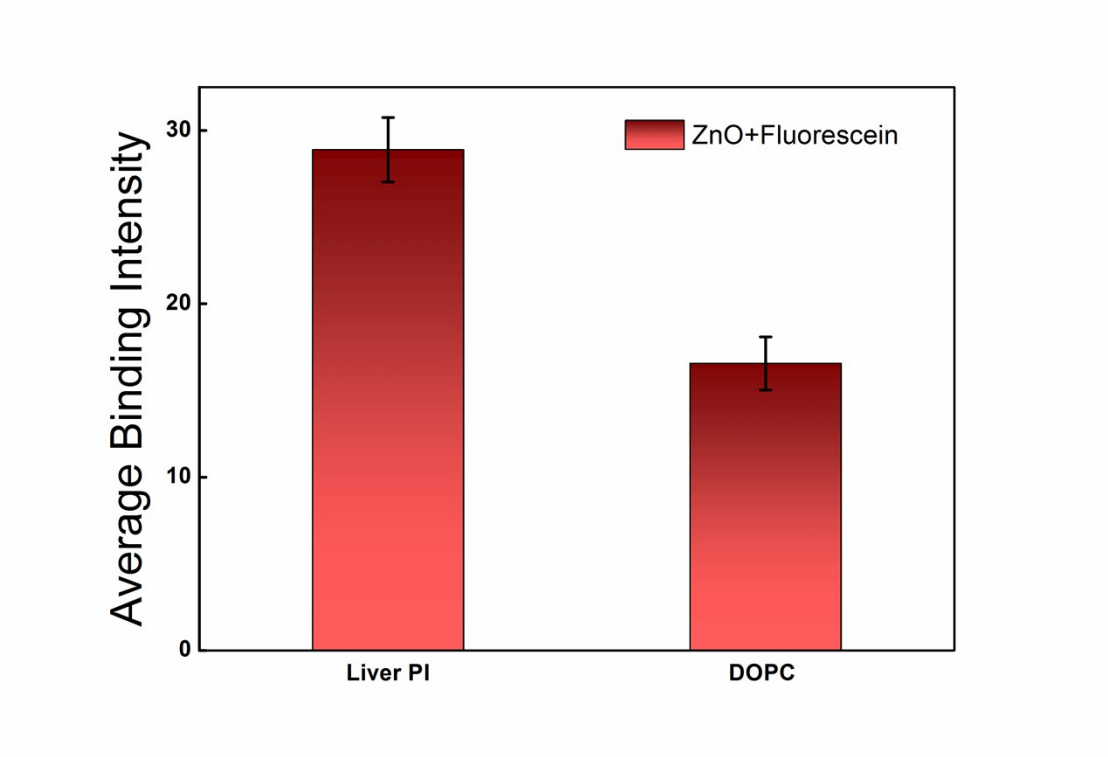

Figure S3: Average binding intensity was extracted using imageJ plugin for oval profile. The only individual lipid membrane found to interact with Fluorescein-ZnONP were liver PI and DOPC. With the intensity for liver PI being higher in comparison to DOPC membranes (number of vesicles used is 35, from three independent experiments).

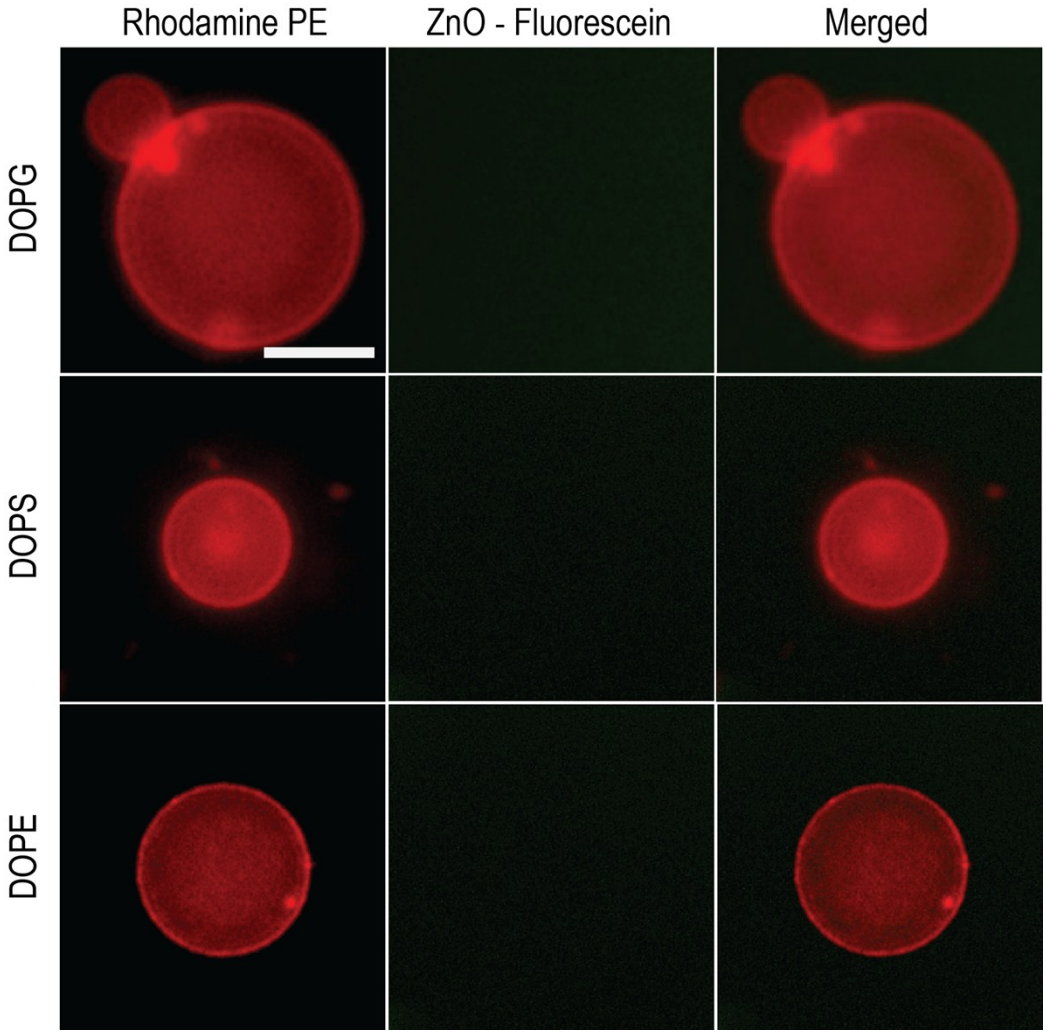

Figure S4 : Lipid specificity of ZnONP.
No interaction between fluorescein-ZnONP and DOPG, DOPS, DOPE was observed as seen from the fluorescence micrograph.

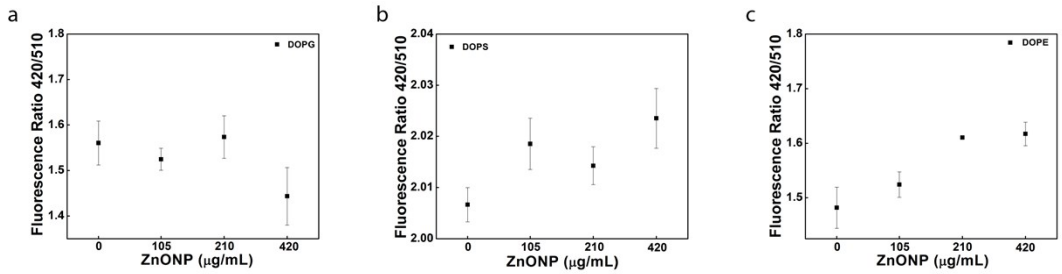

Figure S5: Membrane dipole potential of DOPG, DOPS, DOPE measured using Di-8-ANEPPS. Minor changes in the lipid order were observed upon ZnONP interaction with DOPG, DOPS, DOPE.

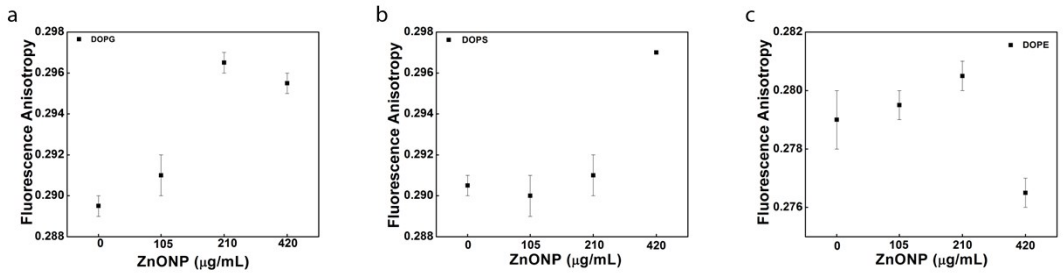

Figure S6 : Membrane Anisotropy of DOPG, DOPS, DOPE measured using Di-8-ANEPPS. Minor changes observed in the membrane anisotropy observed could be due to non-specific interactions.

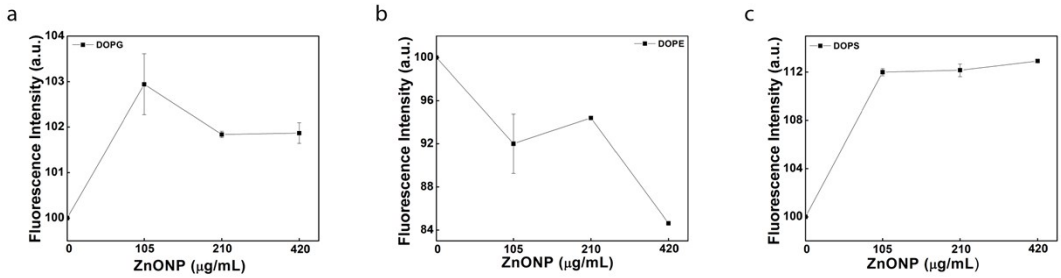

Figure S7: Fluorescence Intensity of DOPG, DOPS, DOPE measured using Di-8-ANEPPS. This gives an idea about the environment surrounding the dye hydrophobic/hydrophilic (Di-8-ANEPPS). Minor changes were observed in the fluorescence intensity of the dye.

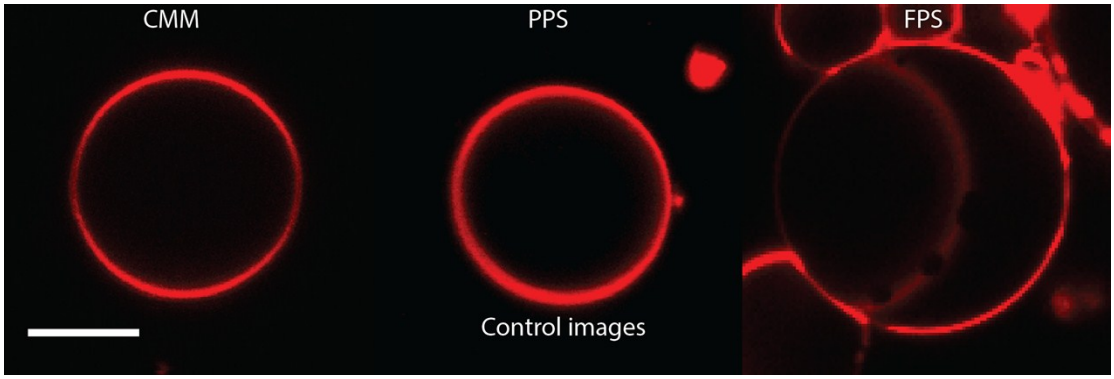

Figure S8: Absence of phase separation in the absence of ZnONP. Absence or delayed mild phase separation for CMM, PPS and FPS likely due to photoinduction even in the absence of ZnONP. Acquisition time was ~ 4 minutes.

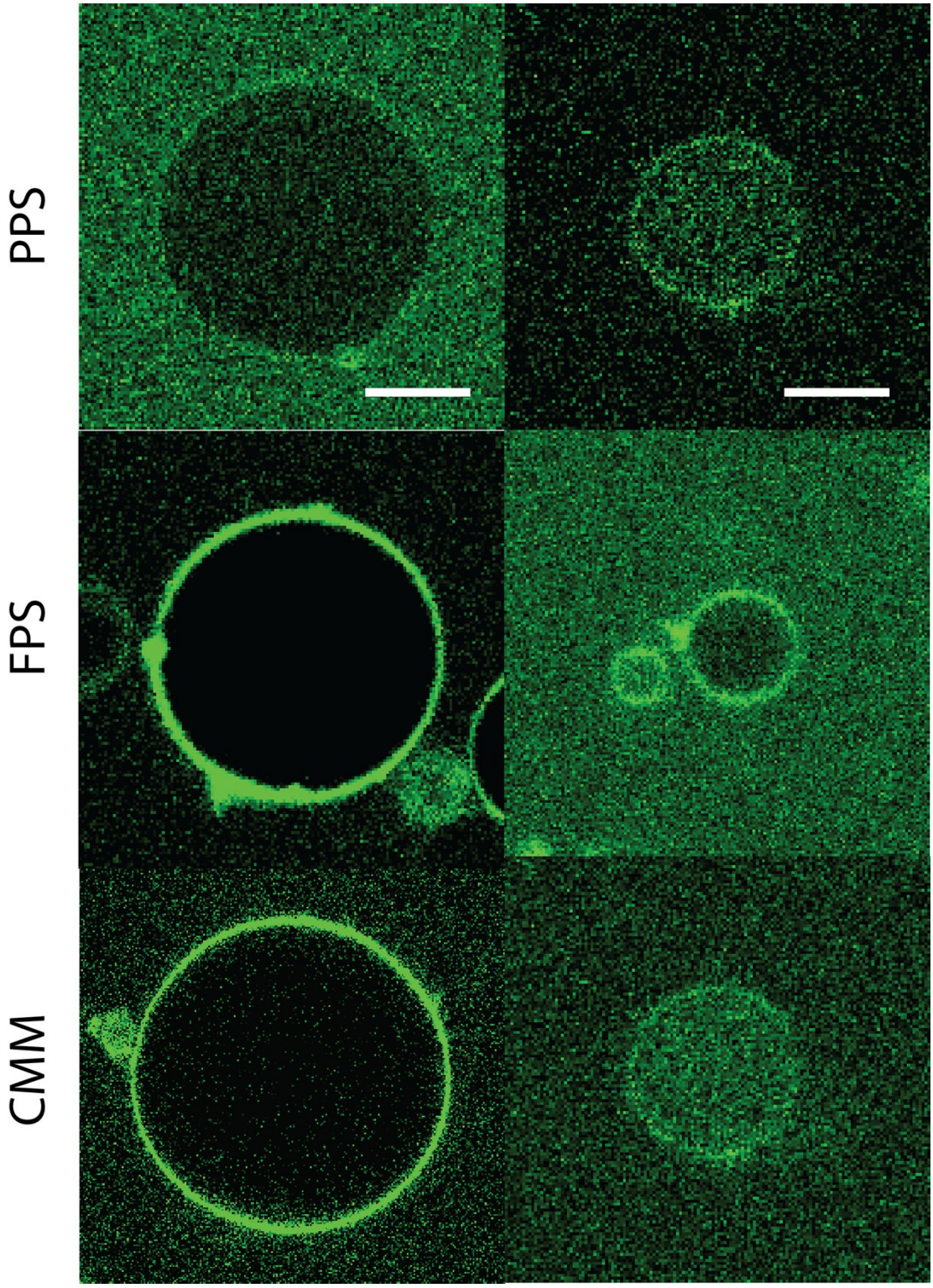

Figure S9: Representative images for internalization and size dependence.
The above image clearly depicts that the internalization is dependent upon the size of the GUV where, greater the size of the GUV the lesser would be the internalization among the same membrane condition. Scale bar, 5 μm.

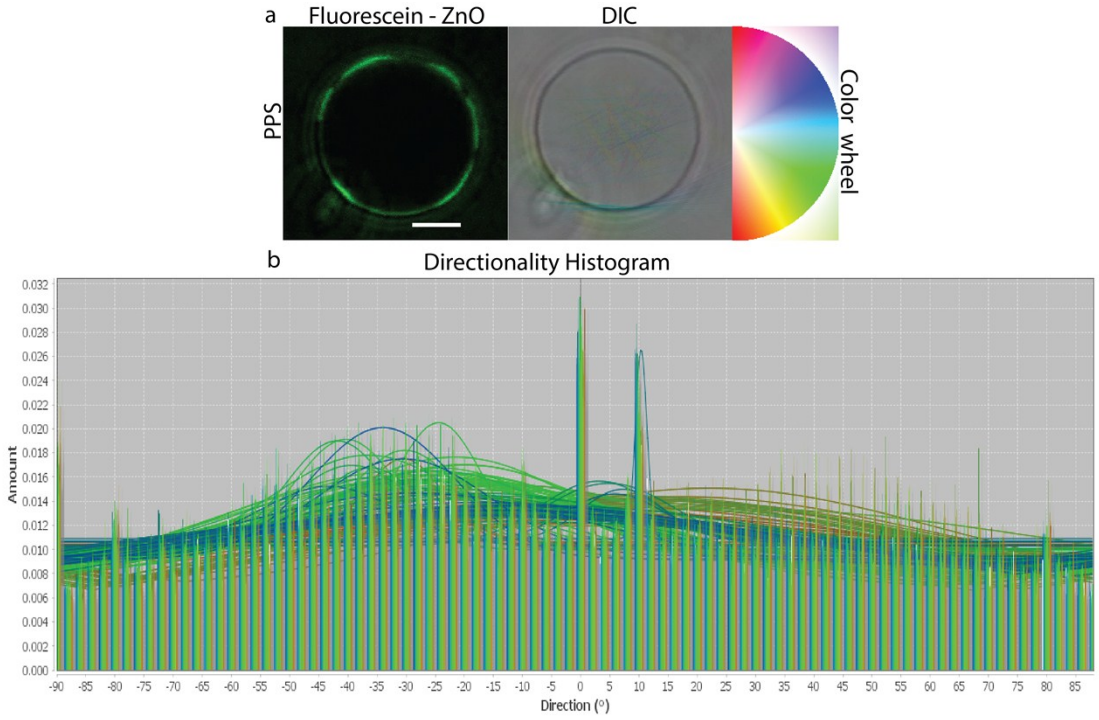

Figure S10: Detection of orientation of intensity fluctuation at membrane edge for partially phase separated condition (PPS). (a) Representative fluorescence and processed differential interference contrast (DIC) image for the time-lapse video of the partially phase separated membrane. The DIC image shows the tangential vectors that detect the preferred orientation of structures in the input image. The color wheel represents the angles. (b) Histogram showing the directionality angles observed on the equatorial plane contour of the GUV for a time-lapse acquisition. This time series of image is not completely isotropic as the histogram suggests presence of several angles suggesting the presence of oscillations in the membranes.

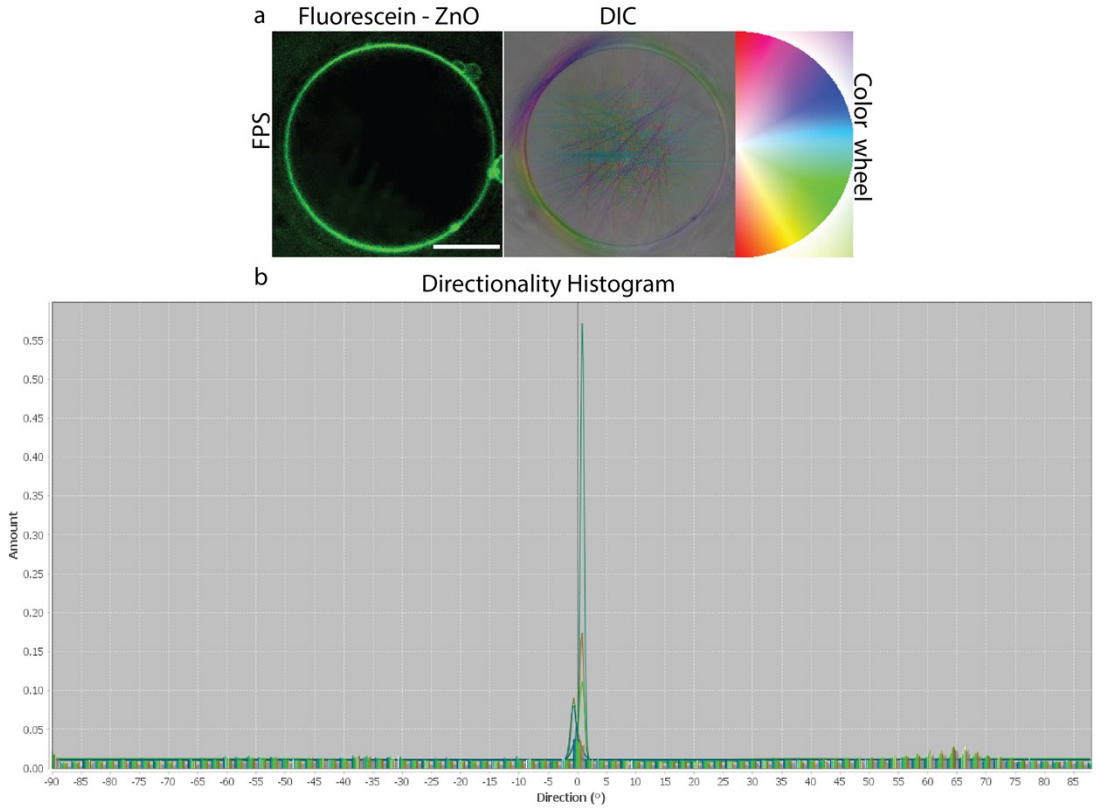

Figure S11: Detection of orientation of intensity fluctuation at membrane edge for fully phase separated condition (FPS). (a) Representative fluorescence and processed differential interference contrast (DIC) image for the time-lapse video of the fully phase separated membrane. The DIC image shows the tangential vectors that detect the preferred orientation of structures in the input image. The color wheel represents the angles. (b) Histogram showing the directionality angles observed on the equatorial plane contour of the GUV for a time-lapse acquisition. This time series of image appears to be isotropic as the histogram is largely flat with peaks around zero degrees suggesting lack of any significant membrane oscillations.

Supplementary Table 1. Membrane dipole potential for varying membrane conditions.

	Membrane composition	**Dipole potential (mV)**
1.	Cell Model Membrane (CMM)	364.66 ± 3.26628
2.	Partially Phase Separated (PPS)	290.31 ± 1.93023
3.	Fully Phase Separated (FPP)	312.91 ± 6.92791

Dipole potential for each test were calculated using the following formula:

$$Dipole\ Potential, \Psi_d = \frac{R + 0.3}{4.3\ X\ 10^{-3}}$$

Where R is the ratio of fluorescence intensities of excitation spectra at 420 nm and 510 nm respectively.[5]

Supplementary Movies

MovieS1: Partially phase separated - ZnO NP binding
MovieS2: Fully phase separated and rigid membrane - ZnO NP binding
MovieS3: FRAP for CMM
MovieS4: FRAP for PPS
MovieS5: FRAP for FPS
MovieS6: Prolonged acquisition of partially phase separated - ZnO NP binding showing the stabilization of the multiple phase separated domains.
MovieS7: Directionality of PPS
MovieS8: Directionality of FPS

References

1. M. Arakha, S. Pal, D. Samantarrai, T. K. Panigrahi, B. C. Mallick, K. Pramanik, B. Mallick and S. Jha, *Sci. Rep.*, 2015, **5**, 14813.
2. X. Zhang, J. Qin, Y. Xue, P. Yu, B. Zhang, L. Wang and R. Liu, *Sci. Rep.*, 2014, **4**.
3. M. Menendez-Miranda, J. M. Costa-Fernández, J. R. Encinar, W. J. Parak and C. Carrillo-Carrion, *Analyst*, 2016, **141**, 1266-1272.
4. E. Gross, R. Bedlack and L. M. Loew, *Biophys. J.*, 1994, **67**, 208-216.
5. T. Starke-Peterkovic, N. Turner, P. L. Else and R. J. Clarke, *American Journal of Physiology-Regulatory, Integrative and Comparative Physiology*, 2005, **288**, R663-R670.